Controllable optical switch using a Bose-Einstein condensate in an optical cavity

Shuai Yang,[1,2] M. Al-Amri,[1,3] Jörg Evers,[1] and M. Suhail Zubairy[1,2]
[1]*Max-Planck-Institut für Kernphysik, Saupfercheckweg 1, D-69117 Heidelberg, Germany*
[2]*Institute for Quantum Studies and Department of Physics, Texas A&M University, College Station, Texas 77843, USA*
[3]*The National Center for Mathematics and Physics, KACST, P.O. Box 6086, Riyadh 11442, Saudi Arabia*
(Received 9 November 2010; published 13 May 2011)

The optical bistability of an ultracold atomic ensemble located in a small-volume ultrahigh-finesse optical cavity is investigated. We find that a transverse pumping field can be used to control the bistable behavior of the intracavity photons induced by the input pumping along the cavity axis. This phenomenon can be used as a controllable optical switch.

DOI: 10.1103/PhysRevA.83.053821 PACS number(s): 37.30.+i, 42.65.Pc, 42.50.Pq, 37.10.Jk

I. INTRODUCTION

Recently, ultracold atomic ensembles located in a small-volume ultrahigh-finesse optical cavity have been studied from many different points of view. If the cavity resonance is far detuned from the atomic resonance, the dispersive regime is realized. The atom-photon interaction then induces an optical lattice for the atoms and affects their mechanical motion. In turn, the atoms imprint a position-dependent phase shift on the cavity field. This highly nonlocal nonlinearity is quite different from the usual local atom-atom interactions and has been exploited for a number of interesting results such as self-organization of atoms [1–6], optical bistability [7–9], cavity-enhanced super-radiant Rayleigh scattering [10], or the mapping between the atoms' ensemble-cavity system and the canonical optomechanical system [11,12]. Also, the analogy to a Dicke quantum phase transition has been studied [13–17].

The optical bistability of the intracavity photon number is typically studied for a system with only one pumping field, which is along the cavity axis. In this work, we consider a system with transverse pumping also (see Fig. 1). We show that the bistable behavior can be controlled by this transverse pumping field. For low transverse pumping, the intracavity photon number shows clear bistability for a particular range of the input pump along the cavity axis. When increasing the transverse pumping field, the range of the bistable behavior is diminished. In particular, above a critical value of the transverse pumping, the bistable behavior disappears. This result provides the possibility of realizing a controllable optical switch. For this, the two stable branches of the output photon number conditioned on the parallel input field act as the optical switch. The transverse pump can then be used to enable or disable this switch. If the switch is disabled, only one of the two possible switch states can be realized, independent of the input field. We verify the operation of the switch using numerical solutions of the underlying Gross-Pitaevskii (GP) equation, and additionally we interpret the results based on a discrete mode approximation (DMA) method [18].

This paper is organized as follows. In Sec. II, we present the system and the general mean-field description. Then in Sec. III, we focus on the bistable behavior of the intracavity photon number when adding the parallel pump field and show how it is controlled by the perpendicular pump. For this, we apply two methods. The GP equation method provides a full description of the problem and leads to an exact solution, while the DMA method reveals a better physical interpretation. In Sec. IV, the effect of the atom-atom interaction on the bistable behavior is analyzed. In Sec. V, the effect of the parallel pumping on the self-organization phase transition is studied. We briefly summarize the results in Sec. VI.

II. THE SYSTEM

The system we consider is a pure Bose-Einstein condensate (BEC) of N two-level atoms with mass m and transition frequency ω_a located inside a high-Q optical cavity with length L and cavity mode frequency ω_c. For the sake of simplicity, we consider the dynamics in the dimension x along the cavity axis only. The cavity field mode function is then described simply by $\cos(kx)$, with wave number k. The model applies to a cigar-shaped BEC, which is tightly confined in the transverse direction by a strong dipole or magnetic trap, such that the transverse size of the condensate is smaller than the waist of the cavity field. Two external pumping laser fields at frequency ω_p are added as shown in Fig. 1, one along the cavity axis and the other perpendicular to the cavity axis. The atom-pump detuning and the cavity-pump detuning are denoted as $\Delta_a = \omega_a - \omega_p$ and $\Delta_c = \omega_c - \omega_p$, respectively. The two pump fields are polarized along the same axis.

In the large-detuning limit and in the rotating frame at the pump frequency, the Hamiltonian for the condensate system can be written as ($\hbar = 1$) [5]

$$\begin{aligned}\hat{H} = \int dx\,\hat{\Psi}^\dagger(x)\Big[&-\frac{1}{2m}\frac{d^2}{d^2x} + U_0\cos^2(kx)\hat{a}^\dagger\hat{a} \\ &+ \eta_\perp\cos(kx)(\hat{a}^\dagger + \hat{a}) + \frac{g_c}{2}\hat{\Psi}^\dagger(x)\hat{\Psi}(x)\Big]\hat{\Psi}(x) \\ &+ \Delta_c\hat{a}^\dagger\hat{a} + \eta_\parallel(\hat{a}^\dagger + \hat{a}). \end{aligned} \quad (1)$$

Here $\hat{\Psi}^\dagger$ and $\hat{a}^\dagger$ are the creation operators for the atoms and the cavity photons, respectively. The atom-cavity photon interaction induces an additional potential $U_0\cos^2(kx)\hat{a}^\dagger\hat{a}$ for the atoms, where $U_0 = -g_0^2/\Delta_a$ is the maximal light shift per photon that an atom may experience, with g_0 being the atom-photon coupling constant. Scattering between the transverse pump field and the cavity mode is described by $\eta_\perp\cos(kx)(\hat{a}^\dagger + \hat{a})$, where $\eta_\perp = -g_0\Omega_p/\Delta_a$ is the maximum scattering rate, with Ω_p being the Rabi frequency of the transverse pump field. We assume the transverse pump laser

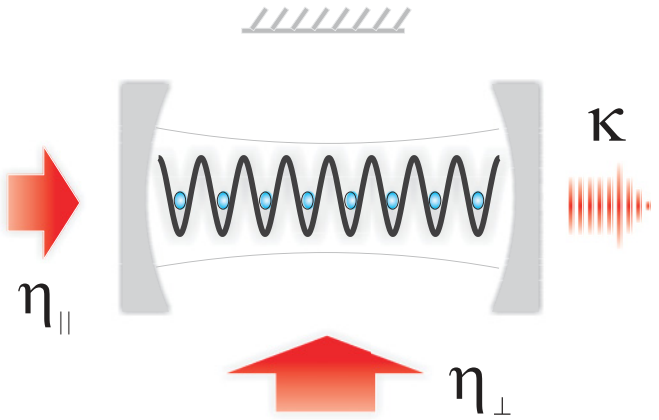

FIG. 1. (Color online) The considered setup of a BEC in a cavity, driven by two pump fields. The transverse pump field is reflected by a mirror indicated in the top of the figure, leading to a standing wave. The characteristics of the pump fields control whether or not the cavity-BEC system exhibits optical bistability.

to be homogeneous along the cavity axis and therefore Ω_p is taken to be constant. $\eta_\parallel$ is the field amplitude of the parallel driving laser and g_c is the atom-atom interaction strength.

In the mean-field approximation, we take the matter-wave field and the cavity electromagnetic field as classical fields, i.e., $\hat{\Psi}(x,t) \sim \Psi(x,t)$ and $\hat{a} \sim \alpha$. The GP equation for the condensate then becomes

$$i\frac{\partial\Psi(x,t)}{\partial t} = \left[-\frac{1}{2m}\frac{d^2}{d^2x} + U_0\cos^2(kx)|\alpha|^2 + \eta_\perp\cos(kx)(\alpha+\alpha^*) + g_c|\Psi(x,t)|^2\right]\Psi(x,t), \tag{2}$$

and the corresponding equation of motion for the cavity field is

$$\frac{\partial\alpha}{\partial t} = -i\left[\Delta_c + U_0\int dx|\Psi(x,t)|^2\cos^2(kx)\right]\alpha - \kappa\alpha - i\eta_\perp\int dx|\Psi(x,t)|^2\cos(kx) + \eta_\parallel. \tag{3}$$

Here we have included the cavity loss κ, which is the dominant dissipation process since spontaneous emission is suppressed under the large-atom-pump-detuning approximation.

In experiments, the cavity damping is usually much faster than the mechanical motion of the condensate, such that the cavity field can follow the condensate adiabatically. We can, therefore, assume the steady state for the cavity field in Eq. (3), i.e.,

$$\alpha = \frac{\eta_\parallel - i\eta_\perp\int dx|\Psi(x,t)|^2\cos(kx)}{i[\Delta_c + U_0\int dx|\Psi(x,t)|^2\cos^2(kx)] + \kappa}. \tag{4}$$

Substituting Eq. (4) into Eq. (2), we obtain a highly nonlocal and nonlinear GP equation. We choose the imaginary-time propagation method [19] to solve this equation numerically. The strategy is to first replace the real time t with $\tau = it$. Then we choose a trial function $\psi(x,t)$ for the GP equation solution, which can be expanded as a linear combination of all the eigenfunctions of the Hamiltonian $\hat{H}$,

$$\psi(x,\tau t) = \sum_i \phi_i(x)e^{-iE_it} = \sum_i \phi_i(x)e^{-E_i\tau}. \tag{5}$$

Evolving the state in imaginary time, the excited states with larger E_i will decay exponentially faster than the ground state. After each small step of the propagation along the imaginary time, we normalize the eigenfunction, which eventually leads to an increase of the ground-state contribution of the evolved state. Ideally, after a certain evolution period, only the ground state survives.

III. OPTICAL BISTABILITY

The cavity photon number is given by

$$n = |\alpha|^2 = \frac{\eta_\parallel^2 + [\eta_\perp\int dx|\Psi(x,t)|^2\cos(kx)]^2}{[\Delta_c + U_0\int dx|\Psi(x,t)|^2\cos^2(kx)]^2 + \kappa^2}. \tag{6}$$

The integrals in the above equation depend on the photon number through the GP equation (2). To the lowest order, we can expect a linear dependence. However, Eq. (6) is a third-order equation in n, such that in general three roots exist. This leads to the appearance of bistability. The bistable behavior relative to the parallel pump strength for the case without transverse pumping has been studied in Ref. [18]. In our setup, we add a transverse pumping field, which provides a second source of cavity photons. As studied in Ref. [6], the self-organization mechanism helps the atoms accumulate in the optical potentials generated by the cavity photons. At a certain transition point, the cavity photon number undergoes a sharp change with the increasing transverse pumping field. From this general behavior, we expect that the bistability of the parallel pump will be suppressed if the transverse pumping field alone fills the cavity with enough photons to establish the upper branch of the bistability. In Fig. 2, we plot the cavity photon number as a function of the parallel pumping field with different but fixed perpendicular pumping fields. It is clear that the bistability of the cavity photon number with the change of the parallel pumping field can be controlled by the perpendicular pumping field. This phenomenon provides a candidate for a controllable optical switch, with the parallel pump field as the input and the perpendicular pump field as the control.

In order to interpret the physics behind our findings we introduce, in addition to the numerical GP calculation, the DMA method for the atom modes at the current step [18]. The ground state of the condensate without the pumping field is a homogeneous macroscopic state with zero momentum. The effect of the transverse pumping field is to diffract this ground state into a symmetric superposition of the $\pm\hbar k$ momentum states. By absorption and stimulated emission of cavity photons the condensate can be excited to the superposition of $\pm 2\hbar k$ momentum states from the ground state. Taking into account the lowest order perturbation to the uniform

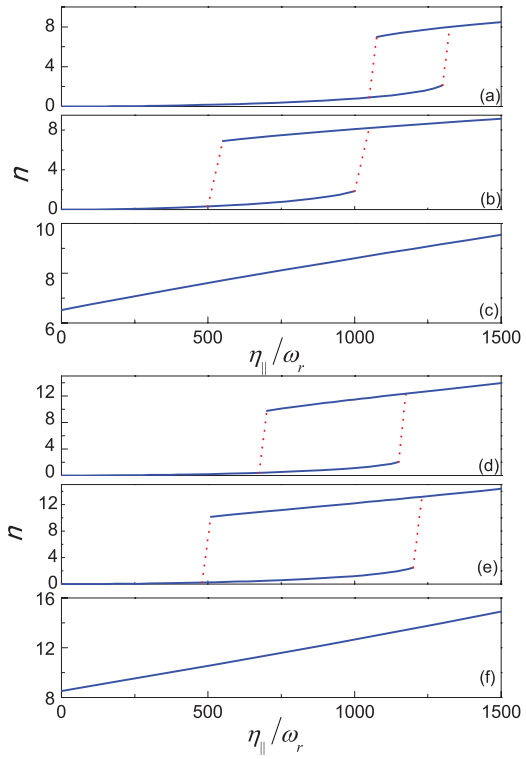

FIG. 2. (Color online) The cavity photon number as a function of the input pump along the cavity axis. For (a) to (c), the parameters are $N = 4.8 \times 10^4$, $\tilde{U}_0 = 0.25$, $\tilde{\delta}_c = 1.2 \times 10^3$, $\tilde{\kappa} = 0.4 \times 10^3$, and (a) $\tilde{\eta}_\perp = 0$, (b) $\tilde{\eta}_\perp = 0.1$, (c) $\tilde{\eta}_\perp = 0.5$. For (d) to (f), the parameters are $N = 1 \times 10^4$, $\tilde{U}_0 = 0.5$, $\tilde{\delta}_c = 1.1 \times 10^3$, $\tilde{\kappa} = 0.2 \times 10^3$, and (a) $\tilde{\eta}_\perp = 0$, (b) $\tilde{\eta}_\perp = 0.4$, (c) $\tilde{\eta}_\perp = 1$. In all cases, we neglect the atom-atom interaction to allow for a direct comparison with the DMA method. The red dotted lines are added to guide the eye.

condensate wave function, we select the subspace expanded by the basis functions

$$\phi_0 = \sqrt{1/L}, \tag{7a}$$

$$\phi_1 = \sqrt{2/L}\cos(kx), \tag{7b}$$

$$\phi_2 = \sqrt{2/L}\cos(2kx), \tag{7c}$$

where L is the length of the cavity. Substituting $\hat{\Psi}(x) = \sum_{i=0}^{2} \phi_i \hat{c}_i$ into the Hamiltonian, we obtain (see the Appendix)

$$\begin{aligned}\hat{H} = {} & \omega_r \hat{c}_1^\dagger \hat{c}_1 + 4\omega_r \hat{c}_2^\dagger \hat{c}_2 + \frac{U_0}{4}\hat{a}^\dagger \hat{a}[\sqrt{2}(\hat{c}_0^\dagger \hat{c}_2 + \hat{c}_2^\dagger \hat{c}_0) \\ & + 2N + \hat{c}_1^\dagger \hat{c}_1] + \frac{\eta_\perp}{2}(\hat{a}^\dagger + \hat{a})[\sqrt{2}(\hat{c}_0^\dagger \hat{c}_1 + \hat{c}_1^\dagger \hat{c}_0) \\ & + (\hat{c}_1^\dagger \hat{c}_2 + \hat{c}_2^\dagger \hat{c}_1)] + \Delta_c \hat{a}^\dagger \hat{a} + \eta_\parallel(\hat{a}^\dagger + \hat{a}),\end{aligned} \tag{8}$$

where $\omega_r = k^2/2m$ is the atomic recoil energy and

$$N = \hat{c}_0^\dagger \hat{c}_0 + \hat{c}_1^\dagger \hat{c}_1 + \hat{c}_2^\dagger \hat{c}_2 \tag{9}$$

characterizes the total number of atoms. Note that if there is no pump field along the cavity axis, then we assume the two modes approximation, i.e., $\hat{c}_2^\dagger = \hat{c}_2 = 0$. In this case, we recover the Dicke Hamiltonian considered in Ref. [17]. On the other hand, if we take the transverse pump field to be zero, which means there is no excitation proportional to $\cos(kx)$, we recover the cavity optomechanical-like Hamiltonian as in Ref. [12].

Applying the mean-field approximation $\hat{c}_i \sim \sqrt{N} X_i$, $\hat{a} \sim \alpha$, the equation of motion for the condensate can be found as

$$\begin{aligned} i\frac{d}{d\tilde{t}}X &= H(\alpha)X \\ &= [H_0 + |\alpha|^2 H_1 + 2\mathrm{Re}(\alpha)H_2]X, \end{aligned} \tag{10}$$

with $X = (X_0, X_1, X_2)^T$ and

$$H_0 = \begin{pmatrix} 0 & 0 & 0 \\ 0 & 1 & 0 \\ 0 & 0 & 4 \end{pmatrix}, \tag{11a}$$

$$H_1 = \frac{\tilde{U}_0}{4}\begin{pmatrix} 0 & 0 & \sqrt{2} \\ 0 & 1 & 0 \\ \sqrt{2} & 0 & 0 \end{pmatrix}, \tag{11b}$$

$$H_2 = \frac{\tilde{\eta}_\perp}{2}\begin{pmatrix} 0 & \sqrt{2} & 0 \\ \sqrt{2} & 0 & 1 \\ 0 & 1 & 0 \end{pmatrix}, \tag{11c}$$

where $\tilde{t} = \omega_r t$, $\tilde{U}_0 = U_0/\omega_r$, and $\tilde{\eta}_\perp = \eta_\perp/\omega_r$ are rescaled dimensionless quantities. Here H_0 is the unperturbed Hamiltonian of the three states, H_1 is the coupling between the homogeneous state and the state ϕ_2 due to the absorption and reemission of cavity photons, and H_2 describes the coupling between ϕ_i and ϕ_{i+1} $(i = 0, 1)$ because of the scattering of perpendicular pumping photons. Since

$$\begin{aligned}\int dx|\Psi(x,t)|^2\cos(kx) &= N\int dx\left[\sqrt{\frac{1}{L}}X_0 + \sqrt{\frac{2}{L}}\cos(kx)X_1 \right. \\ &\quad \left. + \sqrt{\frac{2}{L}}\cos(2kx)X_2\right]^2\cos(kx) \\ &= N(\sqrt{2}X_0X_1 + X_1X_2) \\ &= \frac{1}{\tilde{\eta}_\perp}NX^\dagger H_2 X,\end{aligned} \tag{12}$$

and

$$\begin{aligned}\int dx|\Psi(x,t)|^2\cos^2(kx) &= N\int dx\left[\sqrt{\frac{1}{L}}X_0 + \sqrt{\frac{2}{L}}\cos(kx)X_1 \right. \\ &\quad \left. + \sqrt{\frac{2}{L}}\cos(2kx)X_2\right]^2\cos^2(kx) \\ &= \frac{1}{2}N\left(1 + \frac{1}{2}X_1^2 + \sqrt{2}X_0X_2\right) \\ &= \frac{1}{2}N + \frac{1}{\tilde{U}_0}NX^\dagger H_1 X,\end{aligned} \tag{13}$$

the coherent photon amplitude is

$$\begin{aligned}\alpha &= \frac{\eta_\parallel - iW_0\int dx|\Psi(x,t)|^2\cos(kx)}{i[\Delta_c + U_0\int dx|\Psi(x,t)|^2\cos^2(kx)] + \kappa} \\ &= \frac{\tilde{\eta}_\parallel - iNX^\dagger H_2 X}{i(\tilde{\delta}_c + NX^\dagger H_1 X) + \tilde{\kappa}},\end{aligned} \tag{14}$$

where $\tilde{\delta}_c = (\Delta_c + \frac{1}{2}NU_0)/\omega_r$ and $\tilde{\kappa} = \kappa/\omega_r$.

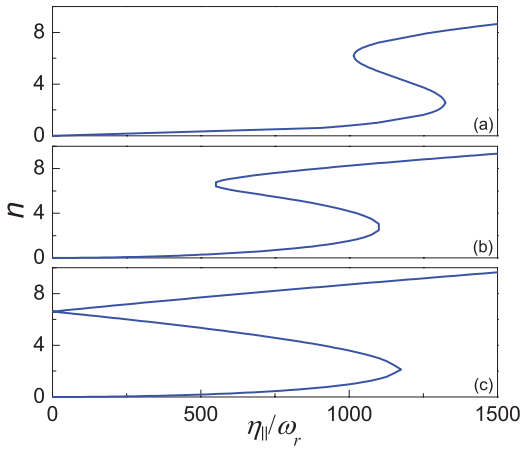

FIG. 3. (Color online) The cavity photon number as a function of the input pump along the cavity axis by the three-level DMA method. The parameters are $N = 4.8 \times 10^4$, $\tilde{U}_0 = 0.25$, $\tilde{\delta}_c = 1.2 \times 10^3$, $\tilde{\kappa} = 0.4 \times 10^3$, and (a) $\tilde{\eta}_\perp = 0$, (b) $\tilde{\eta}_\perp = 0.1$, (c) $\tilde{\eta}_\perp = 0.5$.

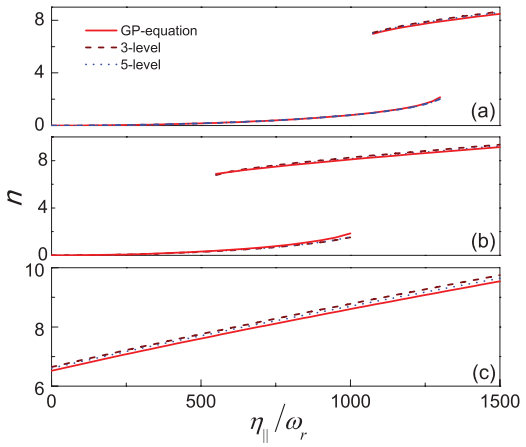

FIG. 4. (Color online) The cavity photon number as a function of the input pump along the cavity axis. The parameters are $N = 4.8 \times 10^4$, $\tilde{U}_0 = 0.25$, $\tilde{\delta}_c = 1.2 \times 10^3$, $\tilde{\kappa} = 0.4 \times 10^3$, and (a) $\tilde{\eta}_\perp = 0$, (b) $\tilde{\eta}_\perp = 0.1$, (c) $\tilde{\eta}_\perp = 0.5$.

Next, we determine the atomic condensate ground state $X_s(t) = X_s e^{-iE_0\tilde{t}}$, where

$$[H_0 + |\alpha|^2 H_1 + 2\mathrm{Re}(\alpha)H_2]X_s = E_0 X_s. \tag{15}$$

This is a nonlinear problem because the Hamiltonian H depends on the eigenstate X_s through α. The procedure is to first take an arbitrary trial photon amplitude α_{tr}, and then solve for the ground state of the Hamiltonian $H(\alpha_{tr})$. Next, we substitute the solution X_s in Eq. (14) and get an output photon amplitude α_{out}. If $\alpha_{\mathrm{out}} = \alpha_{tr}$, a self-consistent solution has been obtained. Figure 3 shows the distinct bistable behavior of the cavity photon number as a function of the input pump along the cavity axis for different transverse pumping fields. Qualitative differences with Fig. 2 arise since the method described above can only solve for the eigenvalues, but it cannot discriminate whether or not the state is stable. In contrast, the GP method leads to stable solutions due to the intrinsic properties of the imaginary time method. If we use the GP results as the start trial photon amplitude, we obtain results as shown in Fig. 4. It can be seen that the DMA and the GP methods agree well. As we include more states in the DMA basis, the results of the approximate method approach those of the exact solution of the GP equation.

When there is no perpendicular pumping, $H_2 = 0$, the cavity photon number

$$n = |\alpha|^2 = \frac{\tilde{\eta}_\parallel{}^2}{(\tilde{\delta}_c + NX^\dagger H_1 X)^2 + \tilde{\kappa}^2}. \tag{16}$$

Here $X^\dagger H_1 X$ is a function of the cavity photon number and can be expanded linearly as $X^\dagger H_1 X \simeq \beta n$, to the lowest order. So

$$n = \frac{n_{in}}{1 + (\tilde{\delta}_c + N\beta n)^2/\tilde{\kappa}^2}, \tag{17}$$

where $n_{in} \equiv \tilde{\eta}_\parallel{}^2/\tilde{\kappa}^2$. This can be mapped exactly to the relation of dispersive optical bistability [20,21]. The scattering of photons due to the atomic gases causes an extra optical length and, thus, a phase change, which depends on the field intensity and produces the bistable states. In Fig. 5(a) we plot the right-hand side of Eq. (16), which can be interpreted as the output cavity photon number n_{out} predicted from Eq. (16) given the input trial photon number n_{tr}. The intersection points of $n_{\mathrm{out}}(n_{tr})$ and the bisection of the first quadrant determined by $n_{\mathrm{out}} = n_{tr}$ provide a graphic solution for the cavity photon number. The bistable behavior emerges when there is more than one intersection. One can easily find that the upper branch corresponds to the intersections on the right side of the peaks, where the number of cavity photons is sufficient to excite the condensate to ϕ_2 with a certain extent [see Fig. 5(b)]. This can be understood from the fact that the bistability comes mainly from the value of β and the quadratic form of the denominator on the right-hand side of Eq. (17).

If perpendicular pumping is added, a new channel for the introduction of cavity photons is set up. It can be easily seen that the perpendicular pumping enters the Hamiltonian,

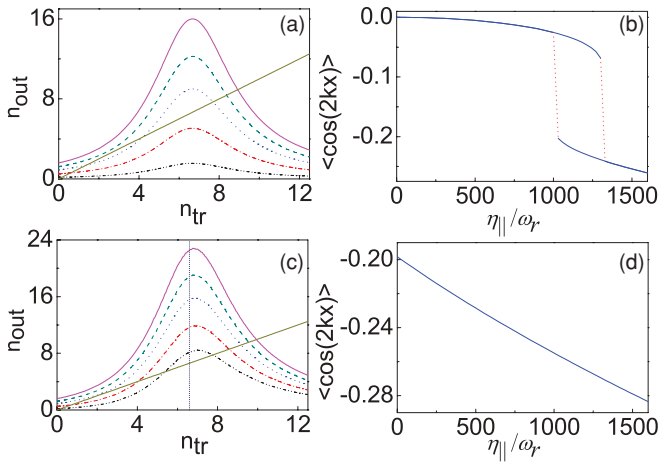

FIG. 5. (Color online) (a) and (c) The cavity output photon number n_{out} as a function of the trial input photon number n_{tr}. (b) and (d) Plots of $\langle\cos(2kx)\rangle$ as a function of the parallel pumping strength. The parameters are $N = 4.8 \times 10^4$, $\tilde{U}_0 = 0.25$, $\tilde{\delta}_c = 1.2 \times 10^3$, $\tilde{\kappa} = 0.4 \times 10^3$, and (a) and (b) $\tilde{\eta}_\perp = 0$ and (c) and (d) $\tilde{\eta}_\perp = 0.5$. The curves in (a) and (c) correspond to $\tilde{\eta}_\parallel = (0.5, 0.9, 1.2, 1.4, 1.6) \times 10^3$, respectively.

like the parallel pumping term, as a displacement operator. The difference is that the pumping rate now depends on the feedback of the atoms and, thus, the cavity photon number, while it is constant for parallel pumping. The reason is that the scattering rate of the perpendicular photons depends on the configuration of the condensate. This point also distinguishes our system from the classical case in which the change of the media's configuration can be neglected and the scattering rate of perpendicular pumping would be a constant too. With the perpendicular field, we find

$$n = \frac{n_{in} + (N\beta' n)^2/\tilde{\kappa}^2}{1 + (\tilde{\delta}_c + N\beta n)^2/\tilde{\kappa}^2}, \tag{18}$$

where $X^\dagger H_2 X \simeq \beta' n$. Comparing Fig. 5(c) with Fig. 5(a), we find that the output photon number as a function of the input photon number, $n_{\rm out}(n_{in})$, is not modified much from the case without parallel pumping. However, the condensate can now be excited from the homogeneous state ϕ_0 to ϕ_2 through scattering of two perpendicular pump photons into the cavity even if no parallel pumping is added. This leads to a nonzero intercept of the vertical axis in Fig. 5(d). Accordingly, potential intersection points located at the left wing of the curves $n_{\rm out}(n_{tr})$ in Fig. 5(c) cannot be accessed if a sufficient number of cavity photons is introduced due to the perpendicular pumping, since this leads to a displacement of the cavity photon number to larger values. In particular, the value of $n_{\rm out}$ at $n_{tr} = 0$ determines a cutoff, which explains the disappearance of the bistability [see Fig. 5(c)].

IV. THE ROLE OF THE ATOM-ATOM INTERACTION

So far, we have neglected the atom-atom interaction by considering the case $g_c = 0$. But in real systems this coupling is usually present and it is helpful in stabilizing the homogeneous phase when the pump power is low. Collisions between atoms with positive scattering lengths tend to diffuse the atoms away from each other. Therefore, the optical lattice generated by the cavity photons can rearrange the atoms only if it is strong enough to overcome the diffusion caused by the atom-atom interaction. Thus, with repulsive atom-atom interactions, more photons are needed to produce a deeper trap to confine the atoms. From this argument we expect that the bistability will still be present with atom-atom interactions, but the parallel pumping field strength needs to be increased to overcome the interaction. This would lead to a shift of the bistability transition to higher values along the parallel pump axis. At the same time, the higher photon number at the transition point also shifts the upper branch upward. This is confirmed in Fig. 6. Since the critical point of self-organization increases with Ng_c as shown in Eq. (22), a stronger transverse input is required to remove the bistability.

V. INFLUENCE OF THE PARALLEL PUMP ON THE DICKE PHASE TRANSITION

By defining

$$\theta = \langle \cos(kx) \rangle, \tag{19a}$$

$$\beta = \langle \cos^2(kx) \rangle, \tag{19b}$$

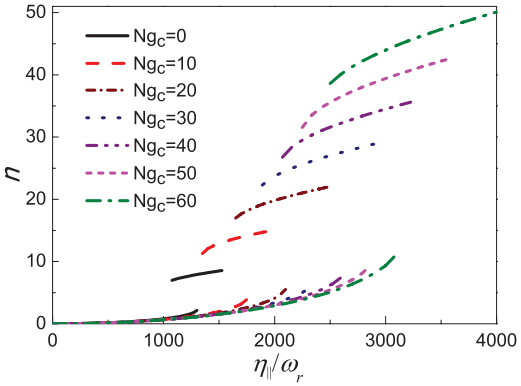

FIG. 6. (Color online) The influence of atom-atom interactions on the bistability. Two lines each with the same line style correspond to the two branches of the bistable behavior for a given value of $Ng_c = 0, 10, 20, 30, 40, 50$, and 60, in units of $\omega_r\lambda/2\pi$ from bottom to top. Other parameters are $N = 4.8 \times 10^4$, $\tilde{U}_0 = 0.25$, $\tilde{\kappa} = 0.4 \times 10^3$, $\tilde{\eta}_\perp = 0$, and $\tilde{\delta}_c = 1.1 \times 10^3$.

the optical lattice potential generated by the cavity photons can be written as

$$\begin{aligned} V(x) &= U_0 \cos^2(kx)|\alpha|^2 + \eta_\perp \cos(kx)(\alpha + \alpha^*) \\ &= V_1 \cos(kx) + V_2 \cos^2(kx), \end{aligned} \tag{20}$$

with

$$V_1 = 2\eta_\perp \frac{\eta_\parallel \kappa - \eta_\perp \theta(\Delta_c + NU_0\beta)}{(\Delta_c + NU_0\beta)^2 + \kappa^2}, \tag{21a}$$

$$V_2 = U_0 \frac{\eta_\parallel^2 + (\eta_\perp \theta)^2}{(\Delta_c + NU_0\beta)^2 + \kappa^2}. \tag{21b}$$

As discussed previously [6] for the case without pumping along the cavity axis, the steady state of the condensate atoms is either a homogeneous distribution or a λ periodic ordered pattern. The two regimes correspond to different transverse pumping strengths and are well separated by a critical point. This sharp transition can be traced back to a self-organization mechanism [6] as follows. If there is no parallel pumping, and if $\Delta_c + NU_0\beta > 0$, the sign of the potential V_1 becomes the opposite of the sign of θ. Therefore, if more atoms happen to be close to the odd (even) sites than to the even (odd) sites due to fluctuations, the produced potential $V_1 \cos(kx)$ will have minima at the odd (even) sites, which attract even more atoms there, leading to an amplification of the fluctuations and, thus, to organization. It follows that apart from the reorganization of the wave function, if the pumping strength is increased over some critical value, the intracavity photon number also shows an abrupt change at the threshold pump power [see Fig. 7(a)]. This phase transition has been shown to be analogous to the Dicke quantum phase transition [16,17]. The critical transition point is determined by

$$\sqrt{N}\eta_\perp = \sqrt{\frac{(\Delta_c + NU_0/2)^2 + \kappa^2}{2\Delta_c + NU_0}}\sqrt{\omega_r + 2Ng_c}. \tag{22}$$

When an extra input pump field is added along the cavity axis, the feedback mechanism works a little differently. The

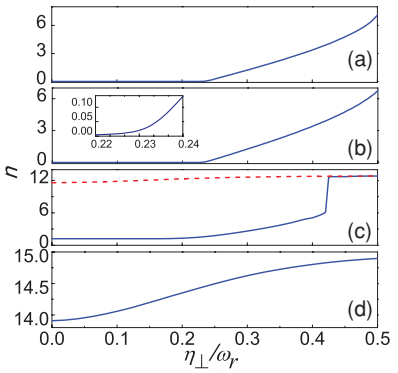

FIG. 7. (Color online) The cavity photon number as a function of the input pump perpendicular to the cavity axis. The parameters are $N = 1 \times 10^4$, $\tilde{U}_0 = 0.5$, $\tilde{\delta}_c = 1.1 \times 10^3$, $\tilde{\kappa} = 0.2 \times 10^3$, $Ng_c = 0$, and (a) $\tilde{\eta}_\parallel = 0$, (b) $\tilde{\eta}_\parallel = 50$, (c) $\tilde{\eta}_\parallel = 1 \times 10^3$, and (d) $\tilde{\eta}_\parallel = 1.5 \times 10^3$.

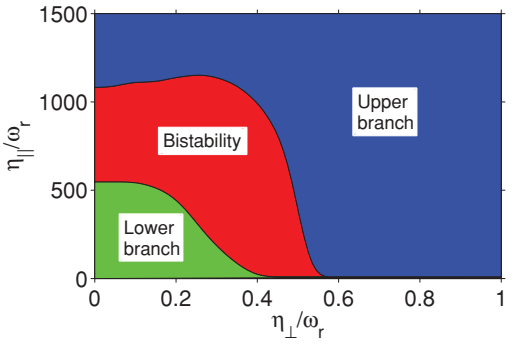

FIG. 8. (Color online) The regions of lower branch, bistability, and upper branch of the cavity photon number. The parameters are $N = 1 \times 10^4$, $\tilde{U}_0 = 0.5$, $\tilde{\delta}_c = 1.1 \times 10^3$, $\tilde{\kappa} = 0.2 \times 10^3$, and $Ng_c = 0$.

parallel pumping provides another channel for cavity photons and forms an additional $\lambda/2$ periodic potential to confine the atoms. Thus, the atoms to the lowest order are in a state ψ_0, which is a coherent superposition of the homogeneous state and ϕ_2. In contrast, without the parallel pump field, the condensate initially is in the homogeneous state only. Furthermore, for the case without the parallel pumping field, the initial homogeneous state is always a self-consistent solution for the combined GP equation and amplitude equation, even with perpendicular pumping. However, this is not true if parallel pumping is added. Then the initial state ψ_0 is not a self-consistent solution for the GP equation as long as perpendicular pumping is added. Therefore, a gradual increase of the perpendicular pumping from zero also leads to a gradual buildup of the λ periodic potential V_1 if a parallel pumping field is applied. From this we expect that no phase transition occurs if parallel pumping is added. This expectation is confirmed by our numerical calculations. Figure 7(b) shows a smooth change of the cavity photon number as we increase $\eta_\perp$ when parallel pumping, $\eta_\parallel = 50$, is added. And, since $\eta_\parallel \kappa > |\eta_\perp \theta(\Delta_c + NU_0\beta)|$ if $\eta_\perp$ is small, the sign of V_1 is positive at the beginning. So the effect of V_1 is to weaken the odd peaks of the $\lambda/2$ periodic potential and strengthen the even peaks. Thus, the atoms will be gradually confined at the odd sites. Alternatively, the sign of $-\eta_\perp \theta(\Delta_c + NU_0\beta)$ will be positive if $\Delta_c + NU_0\beta$ is positive. Then the λ periodic potential will be enhanced as the atoms are attracted to the odd sites. Thus, in this case the atoms will be fixed at the odd sites. We, thus, find that with parallel pumping, the parameters of the system uniquely determine the structure of the condensate after the reorganization. This is in contrast to the case without parallel pumping in which the atoms can be attracted to either of the two equivalent but spatially offset lattice configurations depending on an initial symmetry breaking due to fluctuations.

We recall that bistability can be observed for some particular values of $\eta_\parallel$ and $\eta_\perp$, as explained in Sec. III. Thus, if we increase the pump strength along the cavity axis further, bistability is also expected with the change of transverse pumping [see Fig. 7(c)]. Above a certain critical value of $\eta_\parallel$, the $\lambda/2$ periodic potential will dominate and there is no bistability [see Fig. 7(d)]. So the controllable optical switch can also operate with the parallel pumping as the control and the perpendicular pumping as the signal.

The exact critical point at which the bistable behavior disappears is determined by the highly nonlinear equation

$$\alpha = \frac{\eta_\parallel - i\eta_\perp g(\alpha)}{i[\Delta_c + U_0 f(\alpha)] + \kappa}, \tag{23}$$

where

$$f(\alpha) \equiv \int dx |\Psi(x,t)|^2 \cos^2(kx), \tag{24a}$$

$$g(\alpha) \equiv \int dx |\Psi(x,t)|^2 \cos(kx), \tag{24b}$$

for which only numerical results can be calculated. Close to the critical points, the numerical analysis is complicated by the fact that the ground state and the first excited state become almost degenerate [6]. This increases the likelihood of numerical errors and reduces the efficiency of the algorithm. As a solution, we applied an "adiabatic" evolution of the system, namely, once a wave function is found, we use it as the next trial amplitude after a small parameter change. Figure 8 depicts the regions of the lower branch, bistability, and the upper branch in the parameter space spanned by the two pump fields. We see that for lower pumping fields in both parallel and perpendicular directions, the cavity photon number is mainly in the lower branch. For some intermediate values of the pumping fields, there is bistability for the cavity photon number. If we further increase either the parallel pumping field or the perpendicular pumping field, the cavity photon number is in the upper branch and the bistability disappears. The vertical cross sections of Fig. 8 at $\eta_\perp = 0$, 0.1, and 1.0 and horizontal cross sections at $\eta_\parallel = 0$, 50, 1000, and 1500 coincide with Figs. 2(d)–2(f) and Fig. 7, respectively.

VI. SUMMARY

In conclusion, we have discussed theoretically the bistable behavior of the cavity photon number for a combined cavity-BEC system. We showed that one can use a perpendicular driving field as a control for bistability of the cavity photons

relative to the parallel pump. If no perpendicular driving field is added, the cavity photons show strong bistable behavior for a large range of the parallel pumping field strength. However, if the perpendicular driving exceeds a critical value, this bistability will disappear. Vice versa, we can also use the parallel pumping as a control of the bistability of the perpendicular pumping. While optical bistability with conventional media such as atomic gases and dense crystals has been suggested as a mechanism for an optical switch, this phenomenon may provide a candidate for a controlled optical switch. Further studies are needed for the physics of the dissipation channels and analysis of the switching time of the bistable behavior.

ACKNOWLEDGMENTS

This research is supported by grants from the King Abdulaziz City for Science and Technology (KACST) and NPRP from the Qatar National Research Fund (QNRF). One of us (MSZ) is grateful to the Alexander von Humboldt Foundation for its support.

APPENDIX: DERIVATION OF THE DISCRETE MODE HAMILTONIAN

The derivation of the discrete mode Hamiltonian equation (8) follows from Eq. (1) and Eqs. (7) as

$$
\begin{aligned}
\hat{H} &= \int dx \left[\sqrt{\frac{1}{L}}\hat{c}_0^\dagger + \sqrt{\frac{2}{L}}\cos(kx)\hat{c}_1^\dagger + \sqrt{\frac{2}{L}}\cos(2kx)\hat{c}_2^\dagger\right]\left[-\frac{1}{2m}\frac{d^2}{d^2x} + U_0\cos^2(kx)\hat{a}^\dagger\hat{a} + \eta_\perp\cos(kx)(\hat{a}^\dagger + \hat{a})\right] \\
&\quad\times\left[\sqrt{\frac{1}{L}}\hat{c}_0 + \sqrt{\frac{2}{L}}\cos(kx)\hat{c}_1 + \sqrt{\frac{2}{L}}\cos(2kx)\hat{c}_2\right] + \Delta_c\hat{a}^\dagger\hat{a} + \eta_\parallel(\hat{a}^\dagger + \hat{a}) \\
&= \int dx \left[\sqrt{\frac{1}{L}}\hat{c}_0^\dagger + \sqrt{\frac{2}{L}}\cos(kx)\hat{c}_1^\dagger + \sqrt{\frac{2}{L}}\cos(2kx)\hat{c}_2^\dagger\right]\times\left[\sqrt{\frac{1}{L}}\cos^2(kx)U_0\hat{a}^\dagger\hat{a}\hat{c}_0 + \sqrt{\frac{1}{L}}\cos(kx)\eta_\perp(\hat{a}^\dagger + \hat{a})\hat{c}_0\right. \\
&\quad + \frac{k^2}{2m}\sqrt{\frac{2}{L}}\cos(kx)\hat{c}_1 + \sqrt{\frac{2}{L}}\cos^3(kx)U_0\hat{a}^\dagger\hat{a}\hat{c}_1 + \sqrt{\frac{2}{L}}\cos^2(kx)\eta_\perp(\hat{a}^\dagger + \hat{a})\hat{c}_1 + \frac{4k^2}{2m}\sqrt{\frac{2}{L}}\cos(2kx)\hat{c}_2 \\
&\quad \left. + \sqrt{\frac{2}{L}}\cos^2(kx)\cos(2kx)U_0\hat{a}^\dagger\hat{a}\hat{c}_2 + \sqrt{\frac{2}{L}}\cos(kx)\cos(2kx)\eta_\perp(\hat{a}^\dagger + \hat{a})\hat{c}_2\right] + \Delta_c\hat{a}^\dagger\hat{a} + \eta_\parallel(\hat{a}^\dagger + \hat{a}) \\
&= \frac{U_0}{2}\hat{a}^\dagger\hat{a}\hat{c}_0^\dagger\hat{c}_0 + \frac{U_0}{2\sqrt{2}}\hat{a}^\dagger\hat{a}\hat{c}_2^\dagger\hat{c}_0 + \frac{\eta_\perp}{\sqrt{2}}(\hat{a}^\dagger + \hat{a})\hat{c}_1^\dagger\hat{c}_0 + \frac{k^2}{2m}\hat{c}_1^\dagger\hat{c}_1 + \frac{3U_0}{4}\hat{a}^\dagger\hat{a}\hat{c}_1^\dagger\hat{c}_1 + \frac{\eta_\perp}{\sqrt{2}}(\hat{a}^\dagger + \hat{a})\hat{c}_0^\dagger\hat{c}_1 + \frac{\eta_\perp}{2}(\hat{a}^\dagger + \hat{a})\hat{c}_2^\dagger\hat{c}_1 \\
&\quad + \frac{4k^2}{2m}\hat{c}_2^\dagger\hat{c}_2 + \frac{U_0}{2\sqrt{2}}\hat{a}^\dagger\hat{a}\hat{c}_0^\dagger\hat{c}_2 + \frac{U_0}{2}\hat{a}^\dagger\hat{a}\hat{c}_2^\dagger\hat{c}_2 + \frac{\eta_\perp}{2}(\hat{a}^\dagger + \hat{a})\hat{c}_1^\dagger\hat{c}_2 + \Delta_c\hat{a}^\dagger\hat{a} + \eta_\parallel(\hat{a}^\dagger + \hat{a}) \\
&= \omega_r\hat{c}_1^\dagger\hat{c}_1 + 4\omega_r\hat{c}_2^\dagger\hat{c}_2 + \frac{U_0}{4}\hat{a}^\dagger\hat{a}[\sqrt{2}(\hat{c}_0^\dagger\hat{c}_2 + \hat{c}_2^\dagger\hat{c}_0) + 2N + \hat{c}_1^\dagger\hat{c}_1] + \frac{\eta_\perp}{2}(\hat{a}^\dagger + \hat{a})[\sqrt{2}(\hat{c}_0^\dagger\hat{c}_1 + \hat{c}_1^\dagger\hat{c}_0) + (\hat{c}_1^\dagger\hat{c}_2 + \hat{c}_2^\dagger\hat{c}_1)] \\
&\quad + \Delta_c\hat{a}^\dagger\hat{a} + \eta_\parallel(\hat{a}^\dagger + \hat{a}).
\end{aligned}
\tag{A1}
$$

The atom-atom interaction contains terms such as $\hat{c}_1^\dagger\hat{c}_1\hat{c}_0^\dagger\hat{c}_0$, which mix the discrete modes that we retain as well as other modes that we discard and, therefore, impairs the DMA method. Since the energy scale of the atom-atom interactions is of the order of the chemical potential $\mu = (3g\omega/4)^{2/3}$ (in units of ω_r), we can neglect such interactions on the time scale of $1/\omega_r$ when $\mu \ll 1$ [18]. This condition is fulfilled in a recent experiment [12].

[1] P. Domokos and H. Ritsch, Phys. Rev. Lett. **89**, 253003 (2002).

[2] A. T. Black, H. W. Chan, and V. Vuletić, Phys. Rev. Lett. **91**, 203001 (2003).

[3] J. K. Asbóth, P. Domokos, H. Ritsch, and A. Vukics, Phys. Rev. A **72**, 053417 (2005).

[4] A. Vukics, C. Maschler, and H. Ritsch, New J. Phys. **9**, 255 (2007).

[5] C. Maschler, I. B. Mekhov, and H. Ritsch, Eur. Phys. J. D **46**, 545 (2008).

[6] D. Nagy, G. Szirmai, and P. Domokos, Eur. Phys. J. D **48**, 127 (2008).

[7] S. Gupta, K. L. Moore, K. W. Murch, and D. M. Stamper-Kurn, Phys. Rev. Lett. **99**, 213601 (2007).

[8] J. A. Sauer, K. M. Fortier, M. S. Chang, C. D. Hamley, and M. S. Chapman, Phys. Rev. A **69**, 051804(R) (2004).

[9] S. Ritter, F. Brennecke, K. Baumann, T. Donner, C. Guerlin, and T. Esslinger, Appl. Phys. B **95**, 213 (2009).
[10] S. Slama, S. Bux, G. Krenz, C. Zimmermann, and P. W. Courteille, Phys. Rev. Lett. **98**, 053603 (2007).
[11] K. W. Murch, K. L. Moore, S. Gupta, and D. M. Stamper-Kurn, Nat. Phys. **4**, 561 (2008).
[12] F. Brennecke, S. Ritter, T. Donner, and T. Esslinger, Science **322**, 235 (2008).
[13] R. H. Dicke, Phys. Rev. **93**, 99 (1954).
[14] K. Hepp and E. H. Lieb, Ann. Phys. (NY) **76**, 360 (1973).
[15] Y. K. Wang and F. T. Hioe, Phys. Rev. A **7**, 831 (1973).
[16] K. Baumann, C. Guerlin, F. Brennecke, and T. Esslinger, Nature (London) **464**, 1301 (2010).
[17] D. Nagy, G. Konya, G. Szirmai, and P. Domokos, Phys. Rev. Lett. **104**, 130401 (2010).
[18] J. M. Zhang, F. C. Cui, D. L. Zhou, and W. M. Liu, Phys. Rev. A **79**, 033401 (2009).
[19] P. Muruganandam and S. K. Adhikari, Comput. Phys. Commun. **180**, 1888 (2009).
[20] R. Roy and M. S. Zubairy, Phys. Rev. A **21**, 274 (1980).
[21] P. Meystre and M. Sargent III, *Elements of Quantum Optics*, 3rd ed. (Springer-Verlag, Berlin, 1999).